Optically switchable organic light-emitting transistors

Lili Hou, Xiaoyan Zhang, Giovanni F. Cotella, Giuseppe Carnicella, Martin Herder, Bernd M. Schmidt, Michael Pätzel, Stefan Hecht, Franco Cacialli, Paolo Samorì

Optically switchable organic light-emitting transistors

Lili Hou[1], Xiaoyan Zhang[1,4], Giovanni F. Cotella[2], Giuseppe Carnicella[2], Martin Herder[3], Bernd M. Schmidt[3,5], Michael Pätzel[3], Stefan Hecht[3,*], Franco Cacialli[2,*], Paolo Samorì[1,*]

1 Université de Strasbourg, CNRS, ISIS, 8 alleé Gaspard Monge, 67000 Strasbourg, France. Email: samori@unistra.fr

2 Department of Physics and Astronomy (CMMP Group) and London Centre for Nanotechnology, University College London, Gower Street, London WC1E 6BT, United Kingdom. Email: f.cacialli@ucl.ac.uk

3 Department of Chemistry & IRIS Adlershof, Humboldt-Universität zu Berlin, Brook-Taylor-Str. 2, 12489 Berlin, Germany. Email: sh@chemie.hu-berlin.de

4 Present address: Department of Chemistry and Chemical Engineering, Chalmers University of Technology, 412 96 Gothenburg, Sweden.

5 Present address: Heinrich Heine University Düsseldorf, Insitute for Organic Chemistry and Macromolecular Chemistry, Universitätsstraße 1, 40225 Düsseldorf, Germany.

Organic light-emitting transistors are pivotal components for emerging opto- and nano-electronics applications, such as logic circuitries and smart displays. Within this technology sector, the integration of multiple functionalities in a single electronic device remains the key challenge. Here we show optically switchable organic light-emitting transistors fabricated through a judicious combination of light-emitting semiconductors and photochromic molecules. The irradiation of the solution-processed films at selected wavelengths enables the efficient and reversible tuning of charge transport and electroluminescence simultaneously, with a high degree of modulation (on/off ratios up to 500) in the three primary colours. Different emitting patterns can be written and erased, through a non-invasive and mask-free process, on a length scale of few microns in a single device, thereby rendering this technology potentially promising for optically gated highly-integrated full-colour displays and active optical memory.

Organic light-emitting transistors (OLETs), combining in a single device the functions of light generation of organic light-emitting diodes (OLEDs) with the current modulation (and signal amplification) of organic thin-film transistors (OTFTs), have emerged as a promising new class of devices with significant potential for integrated optoelectronics, smart display technology, and organic lasers[1-5]. The emitting layer of the unencapsulated OLETs is easily accessible for comprehensive optical and electrical investigation of the fundamental physical processes, thereby providing powerful insights into device physics[6,7]. The fabrication of OLETs does not require multiple

metal evaporation steps that are potentially damaging for the interface between electrodes and active layers. As a result, the simplified device architecture enables its potential use in active matrix displays. Furthermore, the position of the recombination region in the channel of ambipolar OLETs can be shifted away from the electrodes as a function of the applied bias, avoiding the metal-induced quenching of excitons[8-10]. Capelli *et al.* recently demonstrated that the performance of OLET can be boosted by exploiting a trilayer heterostructure, surpassing the equivalent OLED efficiency over 100 times[11]. OLETs with performance comparable to display pixels driven by polycrystalline-silicon backplane transistors have been reported, which can be operated at low-voltage and low-power consumption[12].

Besides the efforts devoted to enhance the charge carrier mobility, efficiency, and brightness of OLETs[13-16], the integration of further functionalities into a single device represents another important challenge with the prospect of realizing controllable integrated circuitry[17,18]. Electrically switchable chiral light-emitting transistors (LETs) have been demonstrated, in which the current direction can be used to control the polarization of light from *pn* junctions in tungsten diselenide (WSe_2), which serves as a channel material of LETs[19]. Another example is an all-graphene based light-emitting field-effect device featuring an external electrical bias tuning of the emission spectrum[20]. However, these multifunctional LETs, based on two-dimensional (2D) materials differ in terms of the nature of the charge transport and mechanism of light generation compared to OLETs. The current approach to control "multifunctional"

LETs still relies on external electrical driving. Conversely, optical control offers various advantages, such as non-invasively, high spatial and temporal resolution, and the possibility to tune both wavelength and intensity of the emitted light[21].

Some recent reports demonstrated that it is possible to fabricate optically switchable multifunctional OTFTs[22-24], by blending organic semiconductors with photochromic diarylethenes (DAEs). Upon exposure to light of different wavelength，DAEs can be toggled between two isomers with different electronic properties, and they also show high thermal stability and fatigue resistance during continuous photoswitching[25-27]. Such optically responsive OTFTs exhibited high current switching ratios and large charge carrier mobilities, and have been applied for the fabrication of flexible non-volatile optical memory with over 256 distinct levels[28].

Here we report the fabrication and characterisation of the optically switchable organic light-emitting transistors (OSOLETs), by integrating DAEs into the light-emitting semiconducting layer of OLETs *via* simple solution processing. Both output current and electroluminescence (EL) are simultaneously modulated by irradiating the devices at distinct wavelengths. We demonstrate three classes of OSOLETs emitting over the entire visible spectrum (green, red, and blue), which can reversibly and remotely switch output current and EL on and off *via* visible and UV light irradiation. In addition, emitting patterns within one pixel of the OSOLET can be written and erased easily by using a light beam as an external, non-invasive, and mask-free writing tool

with a spatial resolution down to the far-field diffraction limit, i.e. $\lambda/2NA < 1$ μm (with λ being the wavelength of visible light and NA the numerical aperture of the optical tool used). In view of current minimum pixel sizes, e.g. in the best "retina" displays (~55.5 μm), the present system holds particular potential of reversibly encoding high-density visual information into a single pixel of a high-resolution display.

Mechanism and device fabrication

Three commercially-available semiconducting light-emitting polymers poly(9,9-dioctylfluorene-*alt*-bithiophene) (F8T2), poly[2-methoxy-5-(3',7'-dimethyloctyloxy)-*para*-phenylenevinylene] (MDMO-PPV), and poly(9,9-dioctylfluorene) (F8) were used to fabricate OLETs having fluorescence emission ranging from blue to red (Fig. 1a), thus covering the entire visible spectrum (supplementary Fig. S1 for the absorption and photoluminescence spectra). To enable the optical switching in OLETs, an energetic matching between the photochromic molecules and the emissive materials is required, i.e., the highest occupied molecular orbital (HOMO) levels of the emissive polymers should energetically be positioned in between those of the open and closed DAEs (Fig. 1b). According to cyclic voltammetry (CV) measurements of the light-emitting polymers (see supplementary Fig. S2) and previous studies on DAEs[23,29,30], the HOMO levels of DAEs in their open forms are slightly below the one of the green and blue-emitting hosts (~100 meV) and comfortably below that of MDMO-PPV (~200 meV). Conversely, the HOMO levels of the DAEs in their closed forms are > 600 meV higher than the HOMO of the light-emitting polymers in all three binary components, and thus significant hole trapping is expected for the DAEs in their closed form. In view of the

different HOMO levels of the three polymers responsible for red, green, and blue light emission, we have selected two DAEs, i.e., DAE_tBu and DAE_F (Fig. 1a)[29,30], having high fatigue resistance over repetitive photoswitching cycles in the solid state (Fig. S4). Based on the energetic considerations above, DAE_tBu molecules act as switchable charge traps within the matrix of the emissive F8T2 and MDMO-PPV, whereas the lower HOMO level of DAE_F makes it suitable in combination with the blue emitter (F8).

The OSOLETs were fabricated in a bottom-gate bottom-contact configuration with SiO_2/Si as substrates and the pre-patterned gold interdigitated electrodes as source and drain contacts (Fig. 1c, see device fabrication in the supplementary information). To enhance the charge carrier mobility, self-assembled monolayers (SAMs) of octadecyl-trichlorosilane (OTS) were chemisorbed onto the SiO_2/Si substrates[31,32] prior to spin-coating the solutions of the light-emitting polymers, followed by their thermal annealing at 170 °C to leverage their optoelectronic properties[33]. To avoid thermal degradation of the DAEs at such high temperature, the photochromic molecules were dissolved in solvents orthogonal to those used for the polymers and spun on top of the emissive layer. A gentle post-annealing process was applied to activate the thermal diffusion of DAE molecules into the polymer matrix (80 °C for 1 h in the case of F8T2 and MDMO-PPV, while 40 °C for 1.5 h with regards to F8). The morphologies of the deposited light-emitting polymer/DAE bicomponent films were investigated by atomic force microscopy (AFM, see supplementary Fig. S3). The deposition of DAE_tBu *via* this permeation process did not modify the morphology of F8T2 and no phase

127 separation was observed. Only minor morphology variations were monitored in the case
128 of MDMO-PPV. However, the exposure of neat F8 to both the solvent and thermal
129 treatment, helps the diffusion of DAE_F into F8, and further promotes the formation of
130 supramolecular structures (such as the crystalline phase[34] and the conformational
131 isomer β-phase[35]) of F8, resulting in a rougher morphology (from root-mean-squared
132 roughness R_{rms} = 3.0 nm for the neat F8 film to R_{rms} = 12.3 nm for the F8/DAE_F film)
133 due to the presence of micron-sized islands from the aggregation[36].
134
135 We assessed the retained photoisomerization ability of DAEs in the solid state in
136 the presence of the selected light-emitting polymers for the OSOLETs. UV/visible
137 absorption spectroscopy on the light-emitting polymer/DAE bicomponent films
138 revealed upon UV (312 nm) irradiation the appearance of the typical spectral features
139 in the visible region for the closed DAE isomer that disappear upon green light (> 520
140 nm) irradiation (see supplementary Fig. S5). These observations provide unambiguous
141 evidence that after diffusion into the three polymer matrices the DAEs are still able to
142 undergo reversible photoisomerization.
143
144 **Characteristics of OSOLETs**
145 The performance of OSOLETs in the three primary colours was characterised by
146 using EL spectroscopy as well as transfer curves of current density and luminance *vs.*
147 gate voltage, as summarized in Fig. 2. The light generated within the channel was
148 observed when OSOLETs were in operation, and thereby EL spectra and optical images

149 (inset) of the green, red and blue OSOLETs (channel length L = 2.5 μm and channel
150 width W = 1 cm) were recorded (Figs. 2a-c). The emission peaks of the green and red
151 OSOLETs are located at 540 nm (FWHM = 90 nm) and 630 nm (FWHM = 143 nm),
152 respectively. Two emissive bands appear in the F8/DAE_F based OSOLET with the
153 main peak at 450 nm. The red-shift of EL spectra, compared to that of glassy F8 film
154 with the S_1 to S_0 vibronic peaks at 420 nm, suggests a high fraction of β-phase chain
155 conformations in the F8/DAE_F binary component film[35]. Furthermore, we note the
156 presence of an emission band at longer wavelengths, i.e. a green band, which is
157 common in F8-based emissive devices due to the formation of inter-chain states and/or
158 fluorenone defects[37-40]. Importantly, the emissive bands of the three OSOLETs cover
159 well both the visible region (400-700 nm) and even stretch into the near infrared (NIR)
160 up to 800 nm.
161
162 Although light emission requires bipolar injection, most of the transport of our
163 OSOLETs can be described as essentially unipolar, as inferred from the dependence of
164 the drain current on the applied gate voltage, in line with previous literature on non-
165 switchable OLETs[41-43]. While the holes are evenly distributed within the device channel,
166 light emission provides indeed evidence for electron injection and diffusion ranging to
167 several nm inside the channel. Yet electrons remain minority carriers up to the highest
168 (gate and drain) voltages tested here, as their contribution to the overall current is never
169 appreciable. For this reason, electron transport and light modulation thereof cannot be
170 determined by using the chosen materials (lowest unoccupied molecular orbital

(LUMO) levels listed in Scheme S1). The corresponding light is emitted closely to the electrode in F8T2 based OLET with a longer channel width (L = 20 μm) (see supplementary Fig. S6). However, owing to the resolution of our camera and the narrow channel width of the OSOLETs, the light emission was observed over the entire channel area in the optical images (Figs. 2a-c).

The transfer characteristics of green, red, and blue OSOLETs using DAEs as photo-switchable units were measured (Figs. 2d-f). When the DAEs are in their open forms, the hole mobilities extracted from the transfer characteristics in the saturation regime (see supplementary information for device characterisation) are about 1.5×10^{-3}, 1×10^{-4}, and 5×10^{-7} $cm^2\ V^{-1}s^{-1}$, respectively. For the sake of comparison, the field-effect mobilities in pristine green, red, and blue polymers based OLETs have been measured to be ca. 5×10^{-3}, 2.0×10^{-4}, and 8×10^{-5} $cm^2\ V^{-1}s^{-1}$, respectively (see supplementary Fig. S7). Clearly the hole mobility of F8T2 and MDMO-PPV is slightly reduced due to the scattering (and/or residual trapping) of DAEs in the polymeric matrix. However, the mobility in the blue OSOLETs with the open isomer of DAE_F drops by two orders of magnitude with respect to the one using the neat polymer. It appears that domain boundaries and disordered interphase regions in the F8/DAE_F bicomponent film result in a much rougher morphology, thereby hindering charge transport[44].

The luminance of the OSOLETs was collected simultaneously during measurement of the transfer characteristics (Figs. 2g-i), and it shows a similar trend as drain current

vs. gate voltage (V_g). It should be noted that the pristine F8T2 and MDMO-PPV based OLETs exhibit slightly higher EL intensity as bicomponent ones measured under identical conditions (see supplementary Fig. S7). Interestingly, in the case of F8/DAE_F, despite the reduction of the output current with respect to the pristine material, we observe an increase of luminance, which can be ascribed to the higher photoluminescence efficiency (η_{PL}) of F8 in the so-called β-phase as already reported by Perevedentsev and Hsu et al[35,45]. Therefore, F8T2 and MDMO-PPV based OLETs exhibit a minor variation of EQE, between pristine and bicomponent devices (EQE at $V_g = -80$ V for: MDMO-PPV 2×10^{-3} %, MDMO_PPV/DAE_tBu 6×10^{-3} %, F8T2 0.4×10^{-2} %, and F8T2/DAE_tBu 1.0×10^{-2} %). However, the big change in the morphology leads to a significant increase of the EQE (again at $V_g = -80$ V) of the F8/DAE_F bicomponent device (1.2 %) when compared to the neat F8 device (1.2×10^{-2} %). Although the controlled formation of the β-phase of F8 *via* dipping in solvent/non-solvent mixtures has already been exploited to improve the EQE of F8-based OLEDs[46], no similar investigation has been reported on OLETs yet and we consider this as an additional benefit of combining F8 with DAE_F. A lowering of the operating voltage and enhancement of the brightness is the subject of our future studies, which clearly target technological applications. It can be achieved *via* the careful selection of (i) the light-emitting materials, which should possess high charge carrier mobility and photoluminescence efficiencies, (ii) the dielectric materials, which should exhibit a high gate capacitance, (iii) the optimal device structures, with a shorter channel length

and asymmetric electrodes, and (iv) a hole transport layer and/or an electron transport layer integrated as active component[11-15].

Photoswitching

The remote control *via* light irradiation of the electrical and optical OSOLETs output was investigated. UV (315 nm) irradiation of the OSOLETs yields a significant decrease of both drain current and luminance, which we attribute to ring-closing of the DAEs and subsequent efficient trapping of the majority of carriers. In the case of F8T2/DAE_tBu bicomponent devices, the on/off ratios (the ratio of the current/luminance in the initial state and after UV irradiation) in both transport current and EL exceed 500 (see Figs. 2d and 2g). Such a large degree of modulation is comparable with the reports of photo-programmable OLEDs and non-volatile organic memories[47,48]. A high modulation of the drain current and luminance was also observed for MDMO-PPV/DAE_tBu OSOLET devices (85 % decrease in current and 87 % decrease in luminance, at $V_g = -120$ V, see Figs. 2e and 2h) as well as F8/DAE_F OSOLET devices (65 % decrease in current and 75 % decrease in luminance, at $V_g = -100$ V, see Figs. 2f and 2i). Deeper investigations into the amount of incorporated photochromic molecules, energy levels matching, irradiation dose, and the thickness of active film, will surely enable further improvement of the ON/OFF ratios[22,47-48]. Further irradiation with green (528 nm) light converts the DAEs back to their open form, and leads to full recovery of the initial state in all three-colour OSOLETs. Under the same

irradiation conditions, neat polymer based OLETs did not show any modulation of output current and EL (see supplementary Fig. S7).

It should be noted that the energy transfer from the light-emitting polymers to DAEs in their closed form, favoured by the spectral overlap of the emission of the polymers with the absorption of the DAEs in ring-closed form, can also contribute to the modulation of the intensity of the emitted light. Indeed, a slight modulation of the photoluminescence spectra was detected on the light-emitting polymer/DAE films upon UV and visible irradiation (see supplementary Fig. S9). However, as the switching phenomenon can be observed both on charge transport and light emission, we conclude that energy transfer is not the main operating principle of OSOLETs. Nevertheless, the energy transfer process might help further modulate the intensity of EL, which can be used to explain the larger modulation degree of the luminance than of the current.

The effect of DAE photoswitching on both output current and luminance of the OSOLETs was monitored over three cycles with alternative UV and visible irradiation (Fig. 3). The large modulation of both maximum drain current and luminance of the three-colour OSOLETs, normalized to the initial value for each measurement, is reversible and the optical switching behaviour of OSOLETs is stable over several cycles. Reference OLETs prepared with pristine light-emitting polymers did not show any optically induced modulation, neither on drain current nor on luminance by UV or visible irradiation (see supplementary Fig. S8).

Reversibly write and erase emitting patterns More importantly, since light is used as an external control of our OSOLETs, it is possible to generate emitting patterns with high spatial and temporal resolution on a single transistor as demonstrated by optical images of patterns created and erased in a single OSOLET (Fig. 4). In the initial configuration, the F8T2/DAE_tBu OSOLET was in an all light-emitting on-state (Fig. 4a). Then, the device was irradiated homogenously using UV light yielding a dark state (Fig. 4b). More interestingly, a well-focused green laser (532 nm) can be used to form patterns on the OSOLET with the aid of a microscope. Fig. 4c shows a light-emitting on-area with a pattern of 'H' shape on the same device. Subsequently, the irradiation of the entire device with green light erased the patterns and the all light-emitting on-state can be seen again (Fig. 4d). The second pattern can be written in the same pixel with another step of UV irradiation and followed by one more laser writing step. Fig. 4f exhibits a pattern image of an array of dots in the same area, demonstrating the reversible and reproducible patterning of emissive features up to the micron/sub-micron scale. This demonstration using an optimized combination of photoswitch and emissive polymer illustrates the great potential of our approach to reversibly encode high-density visual information in a single display pixel.

Conclusions

We have fabricated a novel OLET device in which the transport current and electroluminescence, emitting in the range of the three primary colours, can be switched efficiently and reversibly using light as an external stimulus. The active layer in such

optically switchable organic light-emitting transistor comprises an organic light-emitting semiconductor and a photochromic DAE, in which the photo-tunable energy levels of DAEs can either transport or trap the charge carriers, toggled by UV and visible light irradiation. Such a dual external control is achieved through the engineering of the energy levels of the light-emitting polymers and those of the DAEs isomers. We are able to write and erase emitting patterns in a single OSOLET through a non-invasive and mask-free process, with a spatial resolution of a few micrometres, and a response on the microsecond time scale[22]. The stimuli-responsive multifunctional devices proposed in this work are all readily fabricated *via* solution processing, thus potentially transferrable to roll-to-roll compatible or ink-jet printing lines to produce low-cost and flexible stimuli-responsive (nano)electronics on a large scale. Ink-jet printing appears being a most suitable deposition method to fabricate full-colour displays by precisely positioning red, green, and blue emissive inks on each sub-pixel.

In principle, light emission from OLETs in any region of the visible spectrum can be tuned by choosing appropriate photochromic molecules in combination with suitable light-emitting polymers. Future efforts will be directed towards optically switchable OLETs that can be operated at a lower driving power/voltage and yield stronger brightness and a higher ON/OFF ratio. Our approach opens intriguing perspectives towards the development of novel optically gated, integrated full-colour displays, micro-sized light sensors, active optical memories, light controlled inverters, and logic circuitries.

References

1 Muccini, M. A bright future for organic field-effect transistors. *Nature Mater.* **5**, 605–613 (2006).

2 Cicoira, F. & Santato, C. Organic Light Emitting Field Effect Transistors: Advances and Perspectives. *Adv. Funct. Mater.* **17**, 3421-3434 (2007).

3 Santato, C., Cicoira, F. & Martel, R. Spotlight on organic transistors. *Nature Photon.* **5**, 392–393 (2011).

4 Zhang, C., Chen, P. & Hu, W. Organic light-emitting transistors: materials, device configurations, and operations. *Small* **12**, 1252-1294 (2016).

5 Zaumseil, J. & Sirringhaus, H. Electron and ambipolar transport in organic field-effect transistors. *Chem. Rev.* **107**, 1296-1323 (2007).

6 Zaumseil, J., Friend, R. H. & Sirringhaus, H. Spatial control of the recombination zone in an ambipolar light-emitting organic transistor. *Nature Mater.* **5**, 69–74 (2005).

7 Hsu, B. B. Y. *et al.* Control of efficiency, brightness, and recombination zone in light-emitting field effect transistors. *Adv. Mater.* **24**, 1171-1175 (2012).

8 Swensen, J. S., Soci, C. & Heeger, A. J. Light emission from an ambipolar semiconducting polymer field-effect transistor. *Appl. Phys. Lett.* **87**, 253511 (2005).

9 Bisri, S. Z. *et al.* High mobility and luminescent efficiency in organic single-crystal light-emitting transistors. *Adv. Funct. Mater.* **19**, 1728–1735 (2009).

10 Capelli, R. *et al.* Interface functionalities in multilayer stack organic light emitting transistors (OLETs). *Adv. Funct. Mater.* **24**, 5603-5613 (2014).

11 Capelli, R. *et al.* Organic light-emitting transistors with an efficiency that outperforms the equivalent light-emitting diodes. *Nature Mater.* **9**, 496–503 (2010).

12 McCarthy, M. A. *et al.* Low-voltage, low-power, organic light-emitting transistors for active matrix displays. *Science* **332**, 570–573 (2011).

13 Zaumseil, J., Donley, C. L., Kim, J. S., Friend, R. H. & Sirringhaus, H. Efficient top-gate, ambipolar, light-emitting field-effect transistors based on a green-light-emitting polyfluorene. *Adv. Mater.* **18**, 2708–2712 (2006).

14 Gwinner, M. C. *et al.* Highly efficient single-layer polymer ambipolar light-emitting field-effect transistors. *Adv. Mater.* **24**, 2728–2734 (2012).

15 Ullah, M. *et al.* Simultaneous enhancement of brightness, efficiency, and switching in RGB organic light emitting transistors. *Adv. Mater.* **25**, 6213–6218 (2013).

16 Park, S. K. *et al.* Highly luminescent 2D-type slab crystals based on a molecular charge-transfer complex as promising organic light-emitting transistor materials. *Adv. Mater.* **29**, 1701346 (2017).

17 Yang, Y., da Costa, R. C., Fuchter, M. J. & Campbell, A. J. Circularly polarized light detection by a chiral organic semiconductor transistor. *Nature Photon.* **7**, 634–638 (2013).

18 Kim, Y. L. *et al.* Voltage-switchable photocurrents in single-walled carbon nanotube–silicon junctions for analog and digital optoelectronics. *Nature Photon.* **8**, 239–243 (2014).

19 Zhang, Y. J., Oka, T., Suzuki, R., Ye, J. T. & Iwasa, Y. Electrically switchable chiral light-emitting transistor. *Science* **344**, 725–728 (2014).

20 Wang, X. *et al.* A spectrally tunable all-graphene-based flexible field-effect light-emitting device. *Nature Commun.* **6**, 7767 (2015).

21 Zhang, X. Y., Hou, L. L. & Samorì, P. Coupling carbon nanomaterials with photochromic molecules for the generation of optically responsive materials. *Nature Commun.* **7**, 11128 (2016).

22 Orgiu, E. *et al.* Optically switchable transistor via energy-level phototuning in a bicomponent organic semiconductor. *Nature Chem.* **4**, 675–679 (2012).

23 Gemayel, M. E. *et al.* Optically switchable transistors by simple incorporation of photochromic systems into small-molecule semiconducting matrices. *Nature Commun.* **6**, 6330 (2015).

24 Borjesson, K. *et al.* Optically switchable transistors comprising a hybrid photochromic molecule/n-type organic active layer. *J. Mater. Chem. C* **3**, 4156–4161 (2015).

25 Irie, M. & Mohri, M. Thermally irreversible photochromic systems. Reversible photocyclization of diarylethene derivatives. *J. Org. Chem.* **53**, 803–808 (1988).

26 Irie, M., Fukaminato, T., Matsuda, K. & Kobatake, S. Photochromism of diarylethene molecules and crystals: memories, switches, and actuators. *Chem. Rev.* **114**, 12174–12277 (2014).

27 Hou, L., Zhang, X., Pijper, T. C., Browne, W. R. & Feringa, B. L. Reversible photochemical control of singlet oxygen generation using diarylethene photochromic switches. *J. Am. Chem. Soc.* **136**, 910–913 (2014).

28 Leydecker, T. *et al.* Flexible non-volatile optical memory thin-film transistor device with over 256 distinct levels based on an organic bicomponent blend. *Nature Nanotech.* **11**, 769–775 (2016).

29 Herder, M. *et al.* Improving the fatigue resistance of diarylethene switches. *J. Am. Chem. Soc.* **137**, 2738–2747 (2015).

30 Herder, M. *et al.* Light-controlled reversible modulation of frontier molecular orbital energy levels in trifluoromethylated diarylethenes. *Chem. Eur. J.* **23**, 3743–3754 (2017).

31 Salleo, A., Chabinyc, M. L., Yang, M. S. & Street, R. A. Polymer thin-film transistors with chemically modified dielectric interfaces. *Appl. Phys. Lett.* **81**, 4383–4385 (2002).

32 Ito, Y. *et al.* Crystalline ultrasmooth self-assembled monolayers of alkylsilanes for organic field-effect transistors. *J. Am. Chem. Soc.* **131**, 9396–9404 (2009).

33 Lee, T.-W. & Park, O. O. The effect of different heat treatments on the luminescence efficiency of polymer light-emitting diodes. *Adv. Mater.* **12**, 801-804 (2000).

34 Grell, M., Bradley, D. D. C., Inbasekaran, M. & Woo, E. P. A glass-forming conjugated main-chain liquid crystal polymer for polarized electroluminescence applications. *Adv. Mater.* **9**, 798–802 (1997).

35 Perevedentsev, A., Chander, N., Kim, J. S. & Bradley, D. D. C. Spectroscopic properties of poly(9,9-dioctylfluorene) thin films possessing varied fractions of β-phase chain segments: enhanced photoluminescence efficiency via conformation structuring. *J. Polym. Sci. Pol. Phys.* **54**, 1995–2006 (2016).

36 Caruso, M. E., Lattante, S., Cingolani, R. & Anni, M. Microscopic investigation of the poly(9,9-dioctylfluorene) photoluminescence dependence on the deposition conditions by confocal laser microscopy. *Appl. Phys. Lett.* **88**, 181906 (2006).

37 Lim, S. F. *et al.* Suppression of green emission in a new class of blue-emitting PF copolymers with twisted biphenyl moieties. *Adv. Funct. Mater.* **15**, 981–988 (2005).

38 List, E. J. W., Guentner, R., Scanducci de Freitas, P. & Scherf, U. The effect of keto defect sites on the emission properties of polyfluorene-type materials. *Adv. Mater.* **14**, 374-378 (2002).

39 Honmou, Y. *et al.* Single-molecule electroluminescence and photoluminescence of polyfluorene unveils the photophysics behind the green emission band. *Nature Commun.* **5**, 4666 (2014).

40 Gong, X. *et al.* Stabilized blue emission from polyfluorene-based light-emitting diodes: elimination of fluorenone defects. *Adv. Funct. Mater.* **13**, 325-330 (2003).

41 Hepp, A. *et al.* Light-emitting field-effect transistor based on a tetracene thin film. *Phys. Rev. Lett.* **91**, 157406 (2003).
42 Santato, C. *et al.* Tetracene-based organic light-emitting transistors: optoelectronic properties and electron injection mechanism. *Synth. Met.* **146**, 329–334 (2004).
43 Roelofs, W. S. C., Adriaans, W. H., Janssen, R. A. J., Kemerink, M. & Leeuw, D. M. d. Light emission in the unipolar regime of ambipolar organic field-effect transistors. *Adv. Funct. Mater.* **23**, 4133–4139 (2013).
44 Redecker, M., Bradley, D. D. C., Inbasekaran, M. & Woo, E. P. Mobility enhancement through homogeneous nematic alignment of a liquid-crystalline polyfluorene. *Appl. Phys. Lett.* **74**, 1400–1402 (1999).
45 Hsu, B. B. Y. *et al.* Ordered polymer nanofibers enhance output brightness in bilayer light-emitting field-effect transistors. *ACS Nano* **7**, 2344–2351 (2013).
46 Lu, H. H., Liu, C. Y., Chang, C. H. & Chen, S. A. Self-dopant formation in poly(9,9-di-n-octylfluorene) via a dipping method for efficient and stable pure-blue electroluminescence. *Adv. Mater.* **19**, 2574–2579 (2007).
47 Zacharias, P., Gather, M. C., Köhnen, A., Rehmann, N. & Meerholz, K. Photoprogrammable organic light-emitting diodes. *Angew. Chem. Int. Ed.* **48**, 4038–4041 (2009).
48 Scott, J. C. & Bozano, L. D. Nonvolatile memory elements based on organic materials. *Adv. Mater.* **19**, 1452–1463 (2007).

Acknowledgement

We acknowledge funding from the European Commission through the Marie Sklodowska-Curie ITN project iSwitch (GA-642196), the Marie Sklodowska-Curie ITN project SYNCHRONICS (GA-643238), the ERC projects SUPRAFUNCTION (GA-257305) and LIGHT4FUNCTION (GA-308117), the Agence Nationale de la Recherche through the Labex project CSC (ANR-10-LABX-0026 CSC) within the Investissement d'Avenir program (ANR-10-120 IDEX-0002-02), and the International Center for Frontier Research in Chemistry (icFRC) as well as the German Research Foundation (via SFB 765 and SFB 951). FC is a Royal Society Wolfson Research Merit Award holder.

Author contributions

L.H., X.Z., and P.S. conceived the experiments. M.H., B.M.S., M.P., and S.H. synthesized the DAEs. L.H. did UV/visible absorption and PL measurements, and X.Z. performed AFM (the F8/DAE_tBu sample by G.C.) and CV measurements. L.H. and X.Z. designed the devices, performed the electrical experiments and carried out emitting patterns writings. G.F.C., G.C., and F.C designed and built the device characterisation setup. G.F.C., G.C., and L.H. performed the quantitative OLET device characterisation. All authors discussed the results and contributed to the interpretation of data. L.H., X.Z., and P.S. co-wrote the paper with inputs from all co-authors.

Data available statement

The data that support the plots within this paper and other findings of this study are available from the corresponding author upon reasonable request.

Competing interests

The authors declare no competing financial interests

Additional information

Supplementary information is available in the online version of the paper. Reprints and permissions information is available online at www.nature.com/reprints. Correspondence and requests for materials should be addressed to P.S.

Figure captions

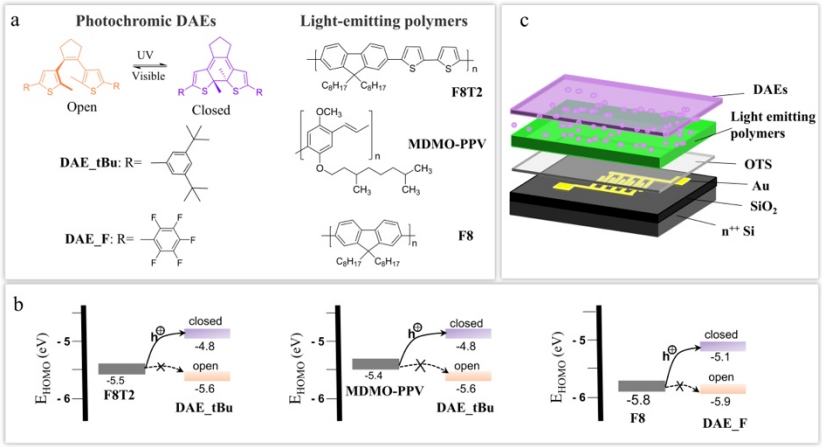

Fig. 1 | Molecules, energetics, and device structure of optically switchable organic light-emitting transistors. a, Chemical structures of photochromic diarylethenes (DAE_tBu and DAE_F) and light-emitting polymers (green: F8T2; red: MDMO-PPV; blue: F8). **b**, Schematic illustration of the switchable charge trapping mechanism of OSOLETs based on the HOMO energy levels of DAEs. As an illustrative example, for F8T2, its hole transport is greatly favoured to the closed form of DAE_tBu but not to the open form of the latter. Thus, there is minimal trapping for the open form, while it is significant for the closed form of DAE_tBu. **c**, Structure of the OSOLETs (substrate, dielectric layer, source and drain electrodes are the same for all the devices, while the light-emitting polymers and DAEs are varied).

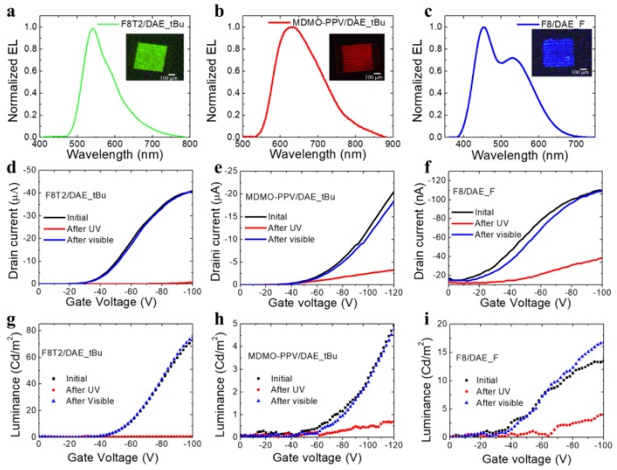

Fig. 2 | Electroluminescence spectra, optical micrographs, and optoelectronic characteristics. a to **c**, EL spectra and emitting images of F8T2/DAE_tBu, MDMO-PPV/DAE_tBu and F8/DAE_F containing OSOLETs. The scale bar in the inset is 100 μm. **d** to **f**, Transfer characteristic curves of F8T2/DAE_tBu OSOLET (V_d = -100 V), MDMO-PPV/DAE_tBu OSOLET (V_d = -120 V) and F8/DAE_F OSOLET (V_d = -100 V), and light-triggered current switching upon UV and visible light irradiation. **g** to **i**, Luminance and light-triggered switching of the luminance in green, red and blue OSOLETs upon UV and visible light irradiation.

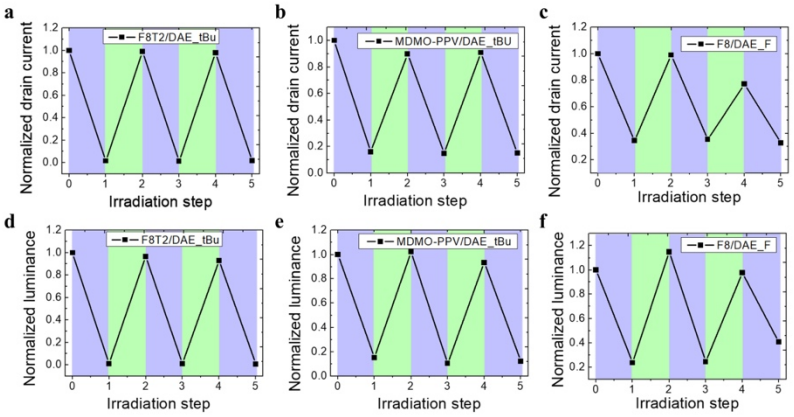

Fig. 3 | Reversible modulation of optically switchable organic light-emitting transistors' current and luminance during irradiation cycles. **a-c** Drain current and **d-f** luminance of green, red, and blue OSOLETs over three irradiation cycles with UV light (315 nm, 0.6 mW, 10 min, violet shaded areas) and visible green light (528 nm,

7 mW, 90 s, green shaded areas). All values are normalized to initial value before any irradiation and the connecting lines serve as ‘guides to the eye’.

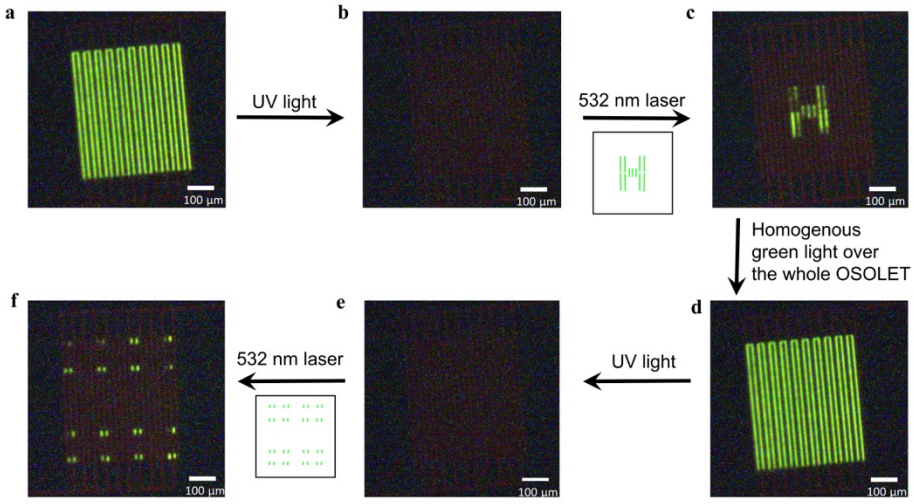

Fig. 4 | Emitting pattern created and erased within a single optically switchable organic light-emitting transistor. **a**, Optical image of a F8T2/DAE_tBu OSOLET device biased with $V_d = V_g = –100$ V. **b**, Optical image of a dark state in the same device after UV light irradiation. **c**, Optical image of an ‘H’ shape emitting pattern from the OSOLET written with a well-focused green laser (532 nm). **d**, Optical image of the second all light-emitting on-state upon homogenous green light irradiation to erase the pattern. **e**, Optical image of the second dark state after homogenous UV irradiation. **f**, Optical image of an array of dots emitting patterns written by the irradiation with a 532 nm laser. The dark area in the pattern is due to the variation of the intensity and/or focus of the laser.